



Angle-resolved SIMS studies of $\text{Al}_x\text{Ga}_{(1-x)}\text{As}$ {001} (2×4) surface reconstruction

S.H. Goss, P.B.S. Kodali, B.J. Garrison, N. Winograd *

Department of Chemistry, The Pennsylvania State University, University Park, PA 16802, USA

Received 16 December 1996; accepted for publication 14 March 1997

Abstract

Angular distributions of Al^+ and Ga^+ ions desorbed by keV particle bombardment have been measured from a modified $\text{Al}_x\text{Ga}_{(1-x)}\text{As}$ {001} (2×4) surface reconstruction. This surface was prepared from the GaAs{001} $c(4 \times 4)$ surface by deposition of one monolayer of aluminum in situ via molecular beam epitaxy. The surface was then annealed to 550 K producing a (2×4) reconstruction. By comparing experimental angular distribution results with molecular dynamics simulations of the bombardment process, we show that Al and Ga segregate into different layers of the prepared (2×4) surface. © 1997 Elsevier Science B.V.

Keywords: Angle-resolved SIMS; Gallium arsenide; Layered resolution; MBE growth; Metal deposition; Single crystal surfaces; Surface reconstruction transformation; (2×4) Reconstruction

1. Introduction

The Al–GaAs interface is often studied due to applications in high technology devices. Moreover it serves as a model system to understand how metals adsorb and grow on a semiconductor surface [1]. The study of metal overlayers on semiconductors is often complicated due to chemical reactions which result in the formation of multi-component interfaces or alloys. Such studies are often further complicated by an incomplete understanding of the atomic structure in the initial surface.

Determination of the relationship between atomic surface structure and electronic property has been sought for many years [2]. For GaAs,

As is known to play a crucial role in the formation of the Fermi level [3] and after Al deposition the As coverage can be related to the resulting Al Schottky barrier height [4]. From a morphological point of view, growth studies of Al on GaAs {001} have shown that the initial reconstruction and Al deposition rate can affect the final orientation of the films [5,6]. A second study of Al growth on GaAs suggests that the surface step density is related to the orientation of Al growth [7]. In each case the initial surface structure strongly influences the structure of the overlayer and ensuing electrical properties. A difficulty with these types of studies is that the initial surface and final structure formed are not well characterized and thus they cannot be easily related to the electronic properties.

In previous work we have identified the atomic positions of clean surfaces and metal overlayers on GaAs with angle-resolved secondary-ion mass

* Corresponding author. Fax: (+1) 814 863.0618;
e-mail: nxw@psuvm.psu.edu

spectrometry (SIMS) [8–10]. It has been shown in these studies that ion distributions from the experiments correspond closely with atom distributions calculated from molecular dynamics (MD) computer simulations. Here we use angle-resolved SIMS to determine the structure of the $\text{Al}_x\text{Ga}_{(1-x)}\text{As}\{001\}$ (2×4) reconstruction produced in situ via molecular beam epitaxy (MBE). The angular distributions of desorbed atoms determined by MD simulations are compared with experimental angular distributions to show that Al and Ga segregate into different layers of the lattice at elevated temperatures.

2. Experimental setup

The experimental setup of our system has been thoroughly described in other work [11,12]. A Riber 2300 MBE chamber is employed to carry out the GaAs synthesis and Al deposition. This chamber is equipped with a reflection high-energy electron diffraction (RHEED) system to monitor the surface reconstructions and growth rate. The growth rate is determined by monitoring RHEED oscillations. One monolayer (ML) is defined in this case to be 6.26×10^{14} atoms/cm² which corresponds to one layer of AlAs. The deposition rate for the Al is 0.067 ML/s. Our modified (2×4) reconstruction was prepared by starting with a GaAs{001} $c(4 \times 4)$ reconstruction and depositing 1 ML of Al at room temperature. After deposition, the $c(4 \times 4)$ reconstruction was annealed to 550 K to yield the (2×4) surface. This conversion of the $c(4 \times 4)$ reconstruction to the (2×4) reconstruction is consistent with previous observations [13,14] and is outlined schematically in Fig. 1. After annealing for 20 min, the sample was cooled to room temperature and transferred under vacuum (1×10^{-10} torr) into the analysis chamber for angle-resolved SIMS experiments. The analysis chamber is equipped with an inert gas ion source for producing the primary Ar^+ ion beam used in these experiments. The detector consists of an energy sector mounted on a quadrupole mass spectrometer to measure the desorbing Ga^+ and Al^+ ions from the surface. The detector is mounted on a rotatable lid such that the sample can be

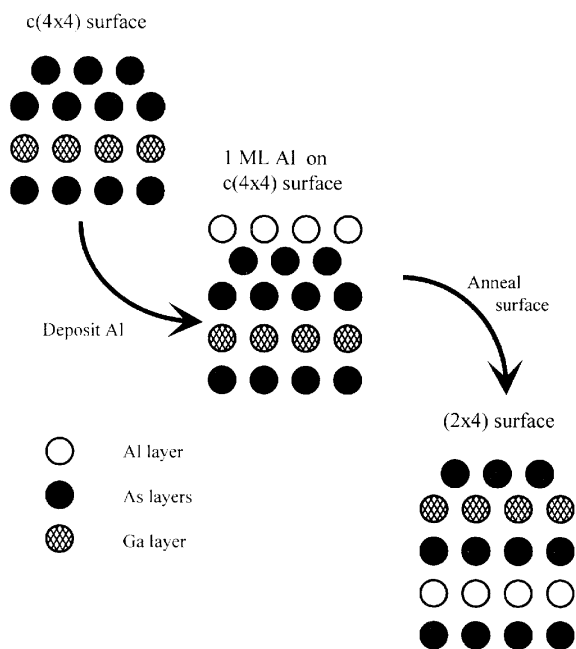


Fig. 1. The schematic outline of how the modified (2×4) reconstruction is formed in situ via MBE. The first step is to form the GaAs{001} $c(4 \times 4)$ reconstruction. The second step is to deposit 1 ML of Al on the $c(4 \times 4)$ reconstruction. The third step is to anneal the surface to 550 K to form the (2×4) reconstruction.

moved independently of the detector. In this work, the primary ion beam is incident normal to the surface. Desorbed secondary ions are detected at various polar (θ) and azimuthal (ϕ) angles. The polar angle is defined by the angle between the normal and the plane of the surface, and the azimuthal angle is defined by rotating the sample around the surface normal. Two important azimuthal angles are shown in Fig. 2.

3. Results and discussion

Molecular dynamics (MD) simulations have been used previously to interpret the peak structure in angle-resolved SIMS investigations of GaAs surfaces [8–10]. The primary use of the MD simulations in this work is to elucidate common trajectories that give rise to features in the angular distribution and to relate those features to atomic positions in the lattice. Moreover, it has been

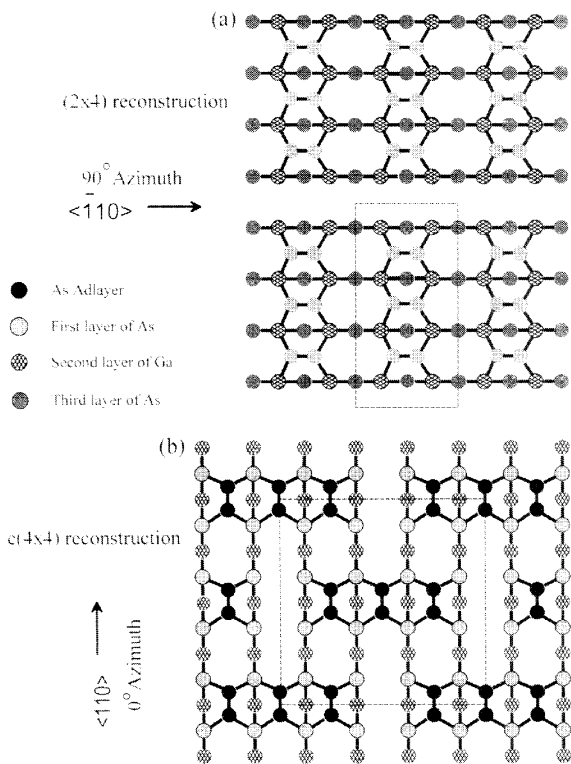


Fig. 2. The two proposed GaAs $\{001\}$ surface reconstructions used in this work: (a) is the three dimer model of the (2×4) reconstruction and (b) is the three dimer model of the $c(4 \times 4)$ reconstruction. The number of As dimers in the (2×4) surface and $c(4 \times 4)$ is not answered in this work since the number of surface dimers does not effect the secondary-ion angular distributions.

shown that the desorption pattern of atoms that eject from each layer can be identified with unique features in the angular distribution. Experimentally it is possible to resolve the mass, energy and ejection angle of the desorbed species. In certain cases it is possible to identify the layer of origin of the desorbed species. In the case of GaAs $\{001\}$, the (2×4) reconstruction is known to have alternating layers of Ga and As, where the even-numbered layers in the lattice are Ga atoms and the odd-numbered layers are As atoms. We would expect the Al atoms to occupy sites that are similar to Ga atoms in the lattice because Al and Ga atoms are in the same group in the periodic table. Hence, Al and Ga atoms would be located in the even-numbered layers. Finally, we note that layer-

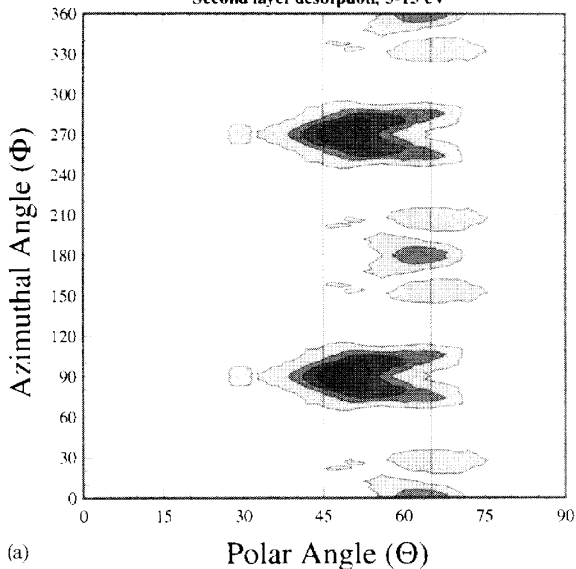
resolved angular distributions from previous MD simulations have yielded useful information about the differences between angular distributions of atoms arising from different layers [15].

The interaction potential used in the MD simulations is a Si potential energy surface (PES) developed by Tersoff [16] and modified by Smith [17]. A Si PES is used due to the unavailability of an effective GaAs PES, and it has been shown in previous work that this Si PES is effective in identifying desorption mechanisms and desorption features for Al–GaAs surfaces [8–12]. The computational details are presented elsewhere and the interested reader should refer to those papers for detailed explanation of the simulations. The MD simulations are performed on a Si $\{001\}$ (2×4) reconstruction to match the experimental $\text{Al}_x\text{Ga}_{(1-x)}\text{As}$ $\{001\}$ (2×4) reconstruction. The crystal used in the simulations is 10 layers thick with 224 atoms per layer, except for the top layer, which only requires 168 atoms to represent the reconstruction. A portion of the crystal with the unit cell outlined is illustrated in Fig. 2(a). According to the MD simulations, the number of dimers on the (2×4) surface does not significantly affect the general behavior of the angular distributions of species desorbed from the second or fourth layer. Hence the main features of the simulations are the same when assuming either two or three dimers per unit cell. The three dimer model used in the simulation presented here was taken from previously observed experimental results for the (2×4) reconstruction [18–20].

The calculated angular distributions for different layers of the $\{001\}$ (2×4) reconstruction are shown in Fig. 3. Only atoms ejected from the second and fourth layers of the crystal are counted since those two layers correspond to the cation layers in the $\text{Al}_x\text{Ga}_{(1-x)}\text{As}$ $\{001\}$ (2×4) reconstruction. The second layer distribution shown in Fig. 3a exhibits a total of four peaks. The dominant pair of peaks occurs at $\Phi = 90$ and 270° , and the minor pair of peaks occurs at $\Phi = 0$ and 180° . The formation of the dominant peak is caused by the third layer atom striking the second layer atom and ejecting the second layer atom. This desorption mechanism is referred to as a Δ_1 mechanism [15]. The formation of the minor peak at $\Phi = 0$ and

Angular Distribution from (2x4)

Second layer desorption, 5–15 eV



Angular Distribution from (2x4)

Fourth layer desorption, 5–15 eV

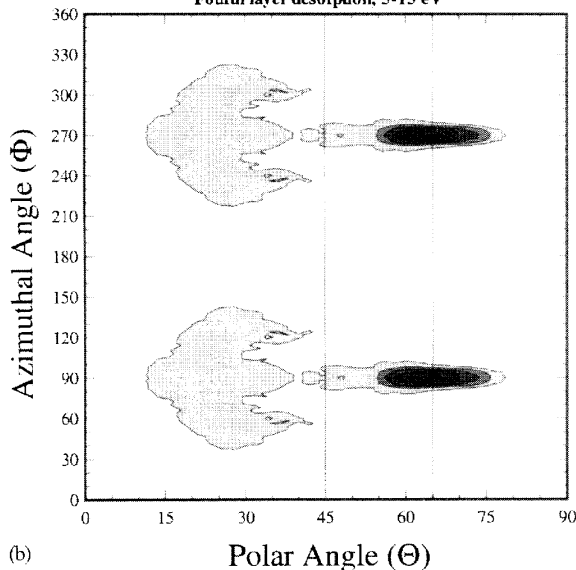


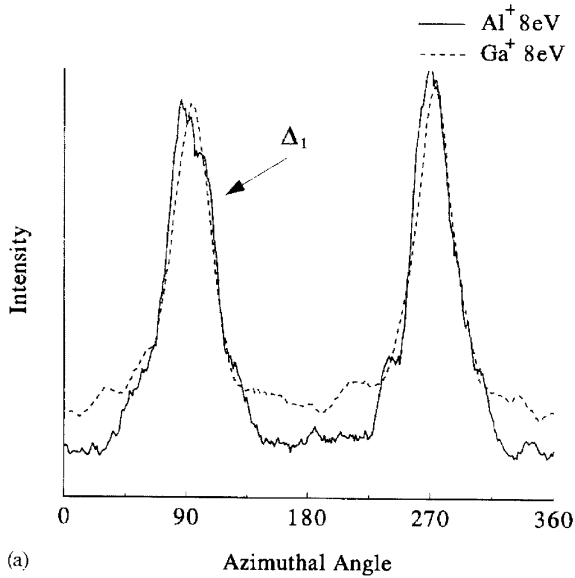
Fig. 3. (a) The MD simulation results for second layer desorption from the $\{001\}$ (2×4) reconstruction. (b) The MD simulation results for fourth layer desorption from the $\{001\}$ (2×4) reconstruction.

180° is caused by a fifth layer atom striking the second layer atom and ejecting the second layer atom. This desorption mechanism is referred to as a Δ_3 mechanism [15]. The angular distribution for the fourth layer is illustrated in Fig. 3b. In this distribution, there is only one set of peaks located at $\Phi = 90^\circ$ and 270° . The formation of these peaks is caused by the fifth layer atom striking the fourth layer atom and ejecting the fourth layer atom. This desorption mechanism is also referred to as a Δ_1 mechanism [15].

By analyzing the second and fourth layer angular distributions of the Si $\{001\}$ (2×4) reconstruction, we now know the angular distribution of the cation layers of the $\text{Al}_x\text{Ga}_{(1-x)}\text{As}$ $\{001\}$ (2×4) reconstruction. Angle-resolved SIMS is performed on this (2×4) reconstruction at two different polar angles for both Al^+ and Ga^+ ions to see if there is any difference in the Al and Ga distributions. Azimuthal distributions of Al^+ and Ga^+ ions for the $\text{Al}_x\text{Ga}_{(1-x)}\text{As}$ $\{001\}$ (2×4) reconstruction are illustrated in Fig. 4. The azimuthal distributions of Al^+ and Ga^+ ions at $\Theta = 45^\circ$ are shown in Fig. 4a. Both the Al^+ and Ga^+ ions at $\Theta = 45^\circ$ have a single pair of peaks in the distribution at $\Phi = 90^\circ$ and 270° . The formation of both sets of peaks is caused by a Δ_1 mechanism. These two distributions are qualitatively similar to the second and fourth layer azimuthal distributions at a polar angle of 45° shown in Fig. 3, as indicated by the line at $\Theta = 45^\circ$. The azimuthal distributions of Al^+ and Ga^+ ions at $\Theta = 65^\circ$ are shown in Fig. 4b. The Al^+ ion distribution has one set of peaks in the scan at $\Phi = 90^\circ$ and 270° , and the formation of these peaks are caused by a Δ_1 mechanism. The Ga^+ ion distribution has two sets of peaks in the scan, one set of peaks at $\Phi = 90^\circ$ and 270° and the second set at $\Phi = 0^\circ$ and 180° . The formation of these peaks at $\Phi = 90^\circ$ and 270° is caused by the Δ_1 mechanism while the formation of these peaks at $\Phi = 0^\circ$ and 180° is caused by the Δ_3 mechanism.

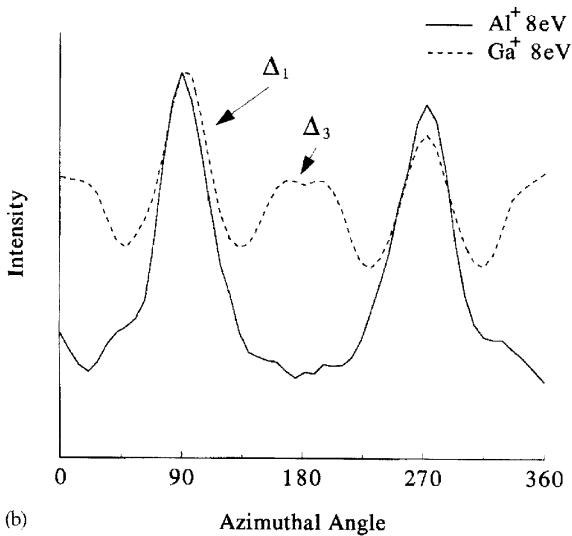
The azimuthal distribution of the Al^+ ions at $\Theta = 65^\circ$ in Fig. 4b is qualitatively similar to the fourth layer azimuthal distribution at $\Theta = 65^\circ$ in Fig. 3b. The azimuthal distribution of the Ga^+ ions at $\Theta = 65^\circ$ in Fig. 4b is qualitatively similar to the second layer azimuthal distribution at $\Theta = 65^\circ$ in Fig. 3a. This qualitative similarity illustrates

Azimuthal scan at 45 degrees
of the modified (2x4) surface



(a)

Azimuthal scan at 65 degrees
of the modified (2x4) surface



(b)

Fig. 4. (a) The azimuthal scan of 8 eV Al⁺ and Ga⁺ ions from the modified (2 × 4) reconstruction at a polar angle (θ) of 45°. (b) The azimuthal scan of 8 eV Al⁺ and Ga⁺ ions from the modified (2 × 4) reconstruction at a polar angle (θ) of 65°. The maximum in each scan has been normalized to unity. These two scans show how the Ga⁺ ion signal changes with angle while Al⁺ ion signal does not change with energy. The arrows indicate the different types of desorption mechanisms present.

that Al and Ga segregate into different layers in the near surface region, where Ga is in the second layer and Al is in the fourth layer. These results do not reveal whether Ga is in the fourth layer and whether Al is in deeper layers below the fourth layer. These results do indicate that Ga outwardly diffuses to the surface and Al inwardly diffuses into the bulk of the GaAs {001} material at the relatively low processing temperature of 550 K.

The driving force for Al and Ga segregation is uncertain at present. It may arise from the increased thermodynamic stability of Al–As bonds over Ga–As bonds. Aluminum has a higher thermodynamic driving force to be bonded to four As atoms in a tetrahedral fashion when compared to Ga. The heat of formation of AlAs is -116.3 kJ/mol versus -70.5 kJ/mol for GaAs [21]. This energy difference may induce the Al to bond in the fourth layer over the second layer because the second layer contains three coordinate sites. A second reason for the segregation of Al and Ga could be due to electrostatic interactions. The electronegativity of Al is lower than Ga (1.5 compared to 1.7) and Al would require more electronic shielding from the electronegative As atoms. The fourth layer would have more electrostatic shielding than the second layer.

4. Conclusion

The results of this work show that the Al is very reactive with the GaAs surface when heated to relatively low processing temperatures of 550 K. These results show that there maybe a fundamental limitation as to how abrupt the Al–GaAs interface can be at normal processing temperatures. We also note that similar migration of group III atoms in the InAs–GaAs system due to annealing has been observed by X-ray photoelectron spectroscopy (XPS) [22]. In that study, thin layers of GaAs were deposited on InAs and then the surface was annealed. Bulk In was observed to migrate into the surface layers upon annealing. This study was unable to obtain layer-resolved resolution because of the limitations of their techniques, but the study does show that the less reactive metal can segregate to the surface.

Finally, we have shown that Al and Ga segregate into different layers in the $\text{Al}_x\text{Ga}_{(1-x)}\text{As}$ $\{001\}$ (2×4) reconstruction produced in situ via MBE. The temperature required to produce this surface is relatively low, suggesting that bulk diffusion occurs well below temperatures required for surface diffusion for GaAs. More theoretical work is needed to understand the factors which drive this atom segregation.

Acknowledgements

We thank J.S. Burnham for helpful discussions regarding this work. The financial support for this work was provided by the National Science Foundation and the Office of Naval Research. The MD calculations were performed on an IBM RS 6000 computer, purchased with a NSF instrumentation Grant and the IBM SUR program.

References

- [1] L.J. Brillson, Surf. Sci. Rep. 2 (1982) 123.
- [2] T. Ohno, Phys. Rev. B 45 (1992) 3516.
- [3] D. Yan, F.H. Pollak, T.P. Chin, J.M. Woodall, Phys. Rev. B 52 (1995) 4674.
- [4] W.I. Wang, J. Vac. Sci. Technol. B 1 (1983) 576.
- [5] P.M. Petroff, L.C. Feldman, A.Y. Cho, R.S. Williams, J. Appl. Phys. 52 (1981) 7317.
- [6] C.J. Kieley, D. Cherns, Phil. Mag. A 59 (1989) 1.
- [7] Y.S. Lou, Y.N. Yang, L.T. Florez, C.J. Palmstrom, Phys. Rev. B 49 (1994) 1893.
- [8] J.S. Burnham, D.E. Sanders, C. Xu, R.M. Braun, S.H. Goss, K.P. Caffey, B.J. Garrison, N. Winograd, Phys. Rev. B 53 (1996) 9901.
- [9] S.H. Goss, P.B.S. Kodali, J.S. Burnham, C. Xu, B.J. Garrison, N. Winograd, to be submitted to Phys. Rev. B.
- [10] S.H. Goss, P.B.S. Kodali, G.L. Fisher, B.J. Garrison, N. Winograd, to be submitted to Phys. Rev. B.
- [11] R. Blumenthal, S.K. Donner, J.L. Herman, R. Terhan, K.P. Caffey, E. Furman, N. Winograd, J. Vac. Sci. Technol. B 6 (1988) 1444.
- [12] K.P. Caffey, R. Blumenthal, J.S. Burnham, E. Furman, N. Winograd, J. Vac. Sci. Technol. B 9 (1991) 2268.
- [13] J.H. Neave, B.A. Joyce, J. Crystal Growth 44 (1978) 387.
- [14] C. Deparis, J. Massies, J. Crystal Growth 108 (1991) 157.
- [15] D.E. Sanders, K.B.S. Prasad, J.S. Burnham, B.J. Garrison, Phys. Rev. B 50 (1994) 5358.
- [16] J. Tersoff, Phys. Rev. B 37 (1988) 6991.
- [17] R. Smith, Harrison D.E., Jr, B.J. Garrison, Phys Rev B 40 (1989) 93.
- [18] D.K. Biegelsen, R.D. Bringans, J.E. Northrup, L.E. Swartz, Phys. Rev. B 41 (1990) 5701.
- [19] M. Sauvage-Simkin, R. Pinchaux, J. Massies, P. Calverie, N. Jedrecy, J. Bonnet, I.K. Robinson, Phys. Rev. Lett. 62 (1989) 563.
- [20] M.D. Pashley, K.W. Haberern, W. Friday, J.M. Woodall, P.D. Kirchner, Phys. Rev. Lett. 60 (1988) 2176.
- [21] R.C. Weast (Eds.), Handbook of Chemistry and Physics, 70th edition, CRC Press, Boca Raton, Florida, 1990.
- [22] M.D. Williams, T.H. Chiu, F.G. Storz, J. Vac. Technol. B 13 (1995) 692.